

Microstructural Characterization and Phase Development at the Interface Between Aluminum Nitride and Titanium After Annealing at 1300°–1500°C

Chia-Hsiang Chiu and Chien-Cheng Lin^{*,†}

Department of Materials Science and Engineering, National Chiao Tung University, Hsinchu 30050, Taiwan

Diffusion couples of aluminum nitride (AlN) and Ti were annealed under an argon atmosphere at temperatures ranging from 1300° to 1500°C for 0.5–36 h. The morphologies, crystal structures, and chemical compositions of the reaction zones at AlN/Ti interfaces were characterized using analytical scanning electron microscopy and analytical transmission electron microscopy. An interfacial reaction zone, consisting of TiN, τ_2 -Ti₂AlN, τ_1 -Ti₃AlN, α_2 -Ti₃Al, and a two-phase (α_2 -Ti₃Al + α -Ti) region in sequence, was observed in between AlN and Ti after annealing at 1300°C. The α_2 -Ti₃Al region revealed equiaxed and elongated morphologies with $[0001]_{\text{equiaxed}} // [\bar{1}100]_{\text{elongated}}$ and $(1010)_{\text{equiaxed}} // (1122)_{\text{elongated}}$. In the two-phase (α_2 -Ti₃Al + α -Ti) region, α_2 -Ti₃Al and α -Ti were found to satisfy the following orientation relationship: $[0001]_{\alpha\text{-Ti}} // [0001]_{\text{Ti}_3\text{Al}}$ and $(1100)_{\alpha\text{-Ti}} // (1100)_{\text{Ti}_3\text{Al}}$. The γ -TiAl and a lamellar two-phase (γ -TiAl + α_2 -Ti₃Al) structure, instead of τ_1 -Ti₃AlN, were found in between τ_2 -Ti₂AlN and α_2 -Ti₃Al after annealing at 1400°C. The orientation relationship of γ -TiAl and α_2 -Ti₃Al in the lamellar structure was identified to be as follows: $[011]_{\text{TiAl}} // [2\bar{1}10]_{\text{Ti}_3\text{Al}}$ and $(1\bar{1}\bar{1})_{\text{TiAl}} // (010)_{\text{Ti}_3\text{Al}}$. Compared with the reaction zone after annealing at 1400°C, the γ -TiAl was not found at the interface after annealing at 1500°C. The microstructural development resulting from isothermal diffusion at 1300°C and subsequent cooling at the interface are explained with the aid of the Ti–Al–N ternary phase diagram and a modified Ti–Al binary phase diagram.

I. Introduction

ALUMINUM NITRIDE has been considered one of the most promising substrate materials for use in semiconductor, microwave, optic, electronic, and other high-performance applications, because of its high thermal conductivity ($\approx 320 \text{ W} \cdot (\text{m} \cdot \text{L})^{-1}$), low dielectric constant (≈ 8.8), a high electric resistivity ($\approx 10^{12}$ – $10^{14} \Omega \cdot \text{cm}$), and coefficient of thermal expansion similar to that of silicon.^{1,2} Meanwhile, Ti is a highly active metal and easily reacts with almost all ceramics,^{3–9} and a high adhesion or bond strength can be achieved by the interface reactions between titanium and the substrate materials. In some applications for microelectronics such as ceramic packaging and metallization,^{10–14} where aluminum nitride is placed in direct contact with titanium, the interfacial properties of AlN and Ti are crucial in determining the quality and reliability of the electric package and its high-temperature applications.

Previous investigations on the interfacial reaction of AlN and Ti have been very limited, most of them concerning the reaction

of AlN with Ti thin films^{15–19} or Ti-containing brazing foils.^{20–22} While available data on the microstructure of the AlN–Ti interfacial reaction zone are often controversial, it is imperative to explore the interdiffusion reactions and mechanisms in the AlN/Ti bonding process in order to make more effective use of AlN and Ti as well.

Some previous studies regarding the thin-film metallization of AlN have been published.^{15–19} As far as the interface reaction between the Ti thin film and the AlN substrate was concerned, Westwood and Notis^{15,16} found the formation of TiN and TiAl₃ at the interface after annealing at 600°C for 30 min in an oxygen-free sample. He *et al.*²³ investigated the interface reactions of Ti thin films with AlN substrate in the temperature range of 600°–800°C using X-ray diffractometry (XRD) and Rutherford backscattering spectroscopy (RBS). They indicated that the TiAl₃ phase was formed at the interface adjacent to the AlN substrate, while TiN, Ti₄N_{3–x}, and Ti₂N were formed above the TiAl₃ layer. Yasurnoto *et al.*¹⁸ deposited a Ti thin film on AlN with radio frequency (rf) sputtering, revealing that under an argon atmosphere, TiAl₃ was formed at 700°C for 60 min, and TiAl₃, Ti₂N, and TiN were detected after annealing at 830°C for 60 min by using XRD. In the study of the interdiffusion and reaction of Ti (thin film) and AlN (substrate) using RBS and transmission electron microscopy (TEM), Imanaka and Notis¹⁹ found Ti₂AlN at the interface after annealing at 800°–950°C. Recently, Pinkas *et al.*²⁴ worked on the early stages of interface reactions between Al and Ti thin films after annealing at 600°C for 1–10 h. They claimed that the AlN decomposed at the AlN/Ti interface and its products, Al and N, reacted with Ti to produce an AlN/Al₃Ti/Ti₂N/Ti₃Al/ α -(Ti,Al)_{ss} phase sequence.

As for the brazing of AlN,^{20–22} Carim and Loehman²⁰ reported that continuous TiN and (Ti, Cu, Al)₆N at the interface of AlN and Ag–Cu–Ti foil were formed after annealing at 900°C for 5–30 min. By using TEM and electron probe microanalysis, Loehman²¹ and Loehman and Tomsia²² indicated that TiN_{0.7} was detected at the interface of AlN and Ag–26.7Cu–4.5Ti after reaction at 900°C for 30 min in an argon atmosphere.

Among other previous studies on the interfacial reaction of AlN and Ti, El-Sayed *et al.*²⁵ characterized the reaction zone microstructure of AlN/Ti (20 or 50 μm thick)/AlN joints after annealing at 1050°–1200°C for 2–20 h in vacuum. The reflection peaks of TiN, Ti₂AlN, Ti₃AlN, and Ti₃Al were observed in the X-ray diffraction spectra taken from the fracture surfaces of annealed joints. Up to 1200°C for 20 h, both TiN_{1–x} and Ti₃AlN did not grow significantly, but the growth kinetics of Ti₃Al followed the parabolic law. Paransky *et al.*^{26–28} investigated the interfacial reactions between AlN particles and the Ti matrix, as well as AlN–Ti diffusion couples, after annealing in the temperature range from 900° to 1100°C using energy-dispersive spectroscopy (EDS) and electron back-scattered diffraction attached to a scanning electron microscope (SEM). A phase sequence of TiN, Ti₃Al_{0.8}N_{0.8}, and Ti₃Al was observed at the interface of Ti and AlN. While the binary nitride TiN and the ternary nitride Ti₃AlN exhibited a complex interpenetrating morphology, a lamellar two-phase region was also

R. Cutler—contributing editor

Manuscript No. 20425. Received April 18, 2005; approved October 26, 2005.

This work was supported by the National Science Council under the contract No. NSC 93-2216-E-009-017.

^{*}Member, American Ceramic Society.

[†]Author to whom correspondence should be addressed. e-mail: chienlin@faculty.nctu.edu.tw

Table I. New Phases Formed in the Interfacial Reaction Zone of AlN/Ti Diffusion Couples

Annealing conditions	Phases						
	TiN	Ti ₂ AlN	Ti ₃ AlN	TiAl	Lamellar structure (TiAl+Ti ₃ Al)	Ti ₃ Al	Two phase region (Ti ₃ Al+Ti)
1300°C/0.5 h	●	x	●	x	x	●	●
1300°C/3 h	●	●	●	x	x	●	●
1300°C/10 h	●	●	●	x	x	●	●
1300°C/36 h	●	●	●	x	x	●	●
1400°C/0.5 h	●	●	x	x	x	●	●
1400°C/3 h	●	●	x	●	●	●	●
1400°C/10 h	●	●	x	●	●	●	●
1400°C/36 h	●	●	x	●	●	●	●
1500°C/0.5 h	●	●	x	●	●	●	●
1500°C/3 h	●	●	x	x	●	●	●
1500°C/10 h	●	●	x	x	●	●	●
1500°C/36 h	●	●	x	x	●	●	●

●, observed; x, none.

observed between Ti₃AlN and Ti₃Al layers after annealing at 1000° and 1100°C.

Many applications of the industrial AlN/Ti joints, such as metallization, brazing, and the composites mentioned above, are determined by the characteristics of the interface between AlN and Ti. In the last few decades, extensive studies have been carried out on the interface reaction between aluminum nitride and titanium. However, the microstructure evolution at the interface has not been elucidated to date, even though a fundamental understanding of reaction and diffusion mechanisms is of great importance for industrial applications and scientific meaning.

The present study is devoted to the microstructural characterization of the interfacial reaction zone in AlN and Ti diffusion couples after annealing at temperatures ranging from 1300° to 1500°C by SEM/EDS and TEM/EDS. We will try to explain the microstructural development at the Ti/AlN interface on the basis of the ternary Al–Ti–N phase diagram and the diffusion paths that connect the phases formed by the reaction between AlN and Ti. The present study is expected to contribute to the understanding of the ternary Ti–Al–N system at high temperatures and to aid in the processing of ceramic–metal joints.

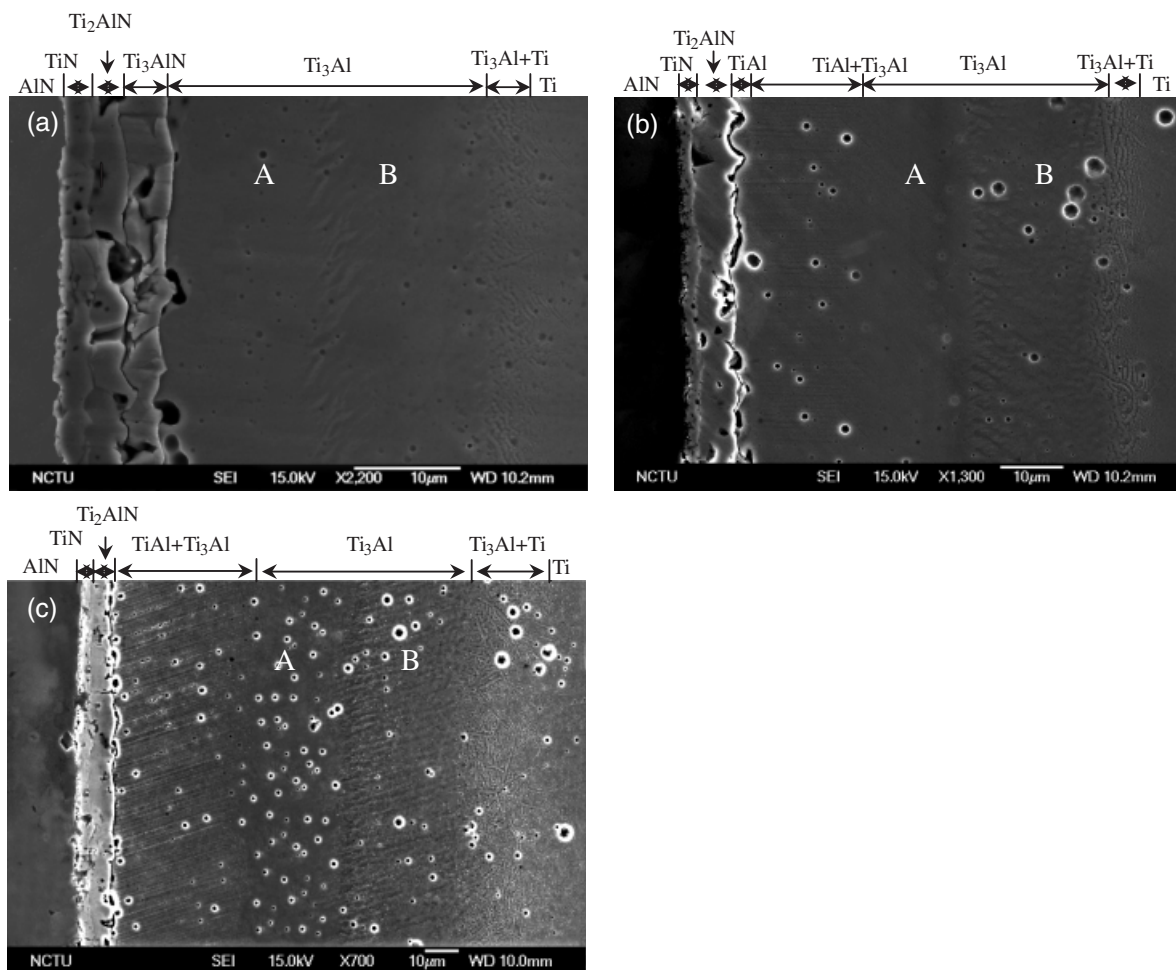


Fig. 1. Scanning electron micrographs of the interface between AlN and Ti after annealing at: (a) 1300°C/36 h; (b) 1400°C/36 h; and (c) 1500°C/36 h.

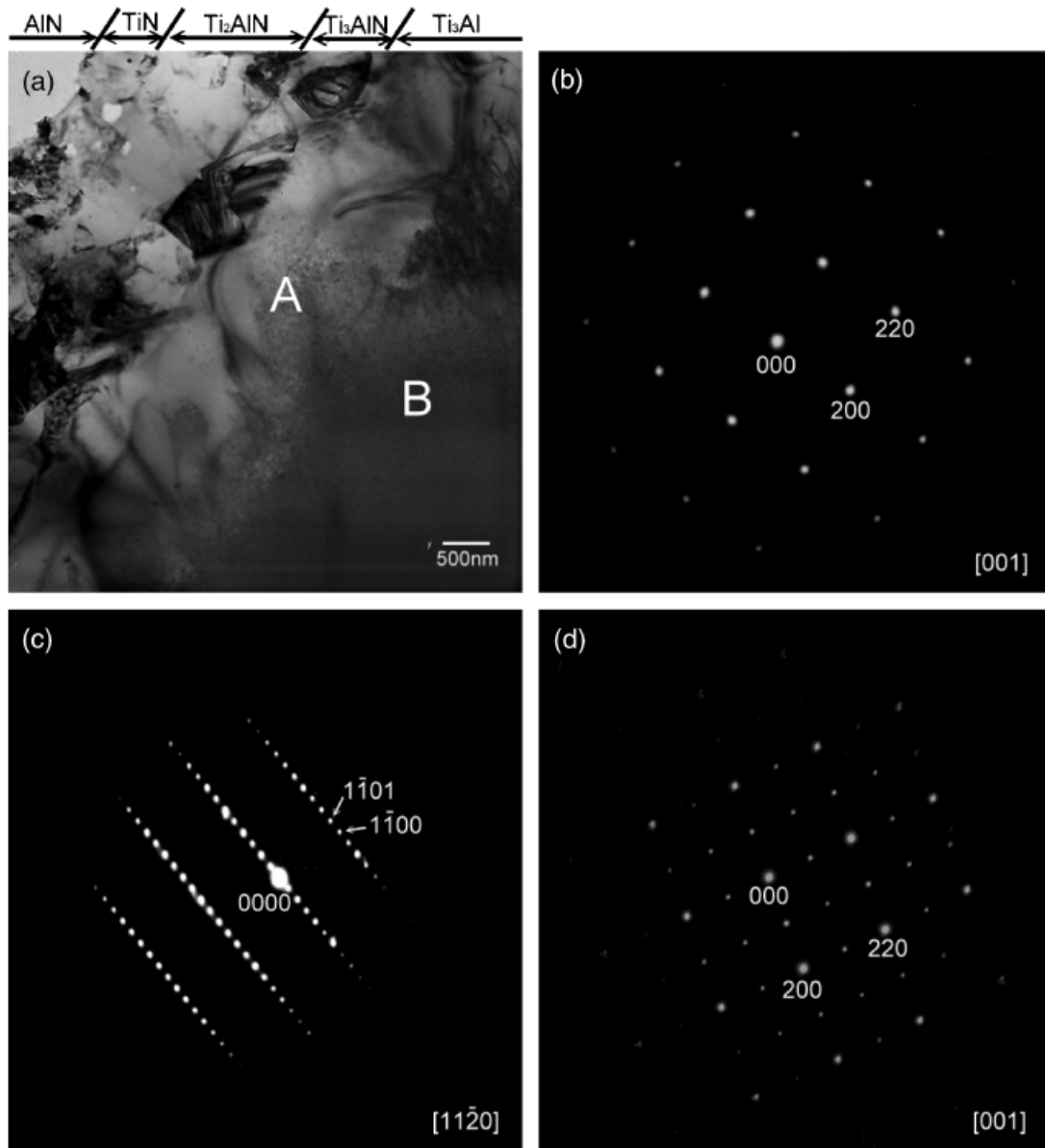


Fig. 2. (a) Bright-field image of the AlN/Ti interface after annealing at 1300°C for 3 h; (b) selected area diffraction pattern (SADP) of TiN, $Z = [001]$; (c) SADP of τ_2 -Ti₂AlN, $Z = [11\bar{2}0]$; and (d) SADP of τ_1 -Ti₃AlN, $Z = [001]$.

II. Experimental Procedure

Highly pure AlN plates (SH-15, Tokuyama Soda Corp., Tokyo, Japan) and Cp-Ti plates (99.7% purity, Alfa Aesar, Ward Hill, MA) were used in this study. All the plates (about 15 mm × 10 mm × 4 mm in dimension) were ground with a diamond (15 μm) matted disk and then polished with a diamond paste (3 μm) and an alumina suspension (1 μm) using a precision polishing machine (Model Minimet 1000, Buehler Ltd., Lake Bluff, IL). The specimens were then rinsed in acetone (ultrasonic bath) and distilled water, and then air-dried.

In order to characterize the microstructure of the Ti/AlN interface, samples were prepared as a sandwich mode with the Ti metal placed in between two pieces of AlN. Then, the samples were annealed in an argon atmosphere (with O₂ < 1 ppm, H₂O < -76 ppm, THC < 0.5 ppm, and N₂ < 3 ppm) under a pressure of 2 MPa at temperatures ranging from 1300° to 1500°C, with a holding time from 0.5 to 36 h, and then the specimen was continuously cooled down to room temperature at a rate of 10°C/min.

The cross-sectional TEM and SEM samples were prepared as follows: each annealed sample was cut into two halves in a direction perpendicular to the interface of AlN/Ti, and then

ground and polished by the standard procedures as mentioned above. The samples were etched with the Kroll reagent (10 mL HF + 30 mL HNO₃ + 60 mL H₂O) in order to emphasize the features of different phases and to remove the deformed surface layer. Thereafter, the samples were rinsed in acetone (ultrasonic bath) and distilled water, and then air dried. To avoid charging, all the SEM samples were coated with a thin layer of platinum (finished preparation of SEM samples). The cross-sectional slab was ground down to an 80–100 μm thickness using a precision polishing machine; then, the sample was thinned to 20–30 μm by dimpling, and finally argon ion milled at 5 kV and 20 μA (finished preparation of TEM samples).

Microstructural characterization of the cross-sections of AlN/Ti was carried out using a high-resolution scanning electron microscope (Model JSM-6500, JEOL, Tokyo, Japan) and an analytical TEM (Model 2000F_x, JEOL). The Cliff-Lorimer standardless technique was used to analyze the compositions of the various phases. The technique was performed on the TEM, equipped with an ultra-thin window EDS detector (Model 9900, EDAX International, Prairie View, IL). A conventional ZAF correction procedure included in the LINK ISIS software was used for the quantitative analyses.

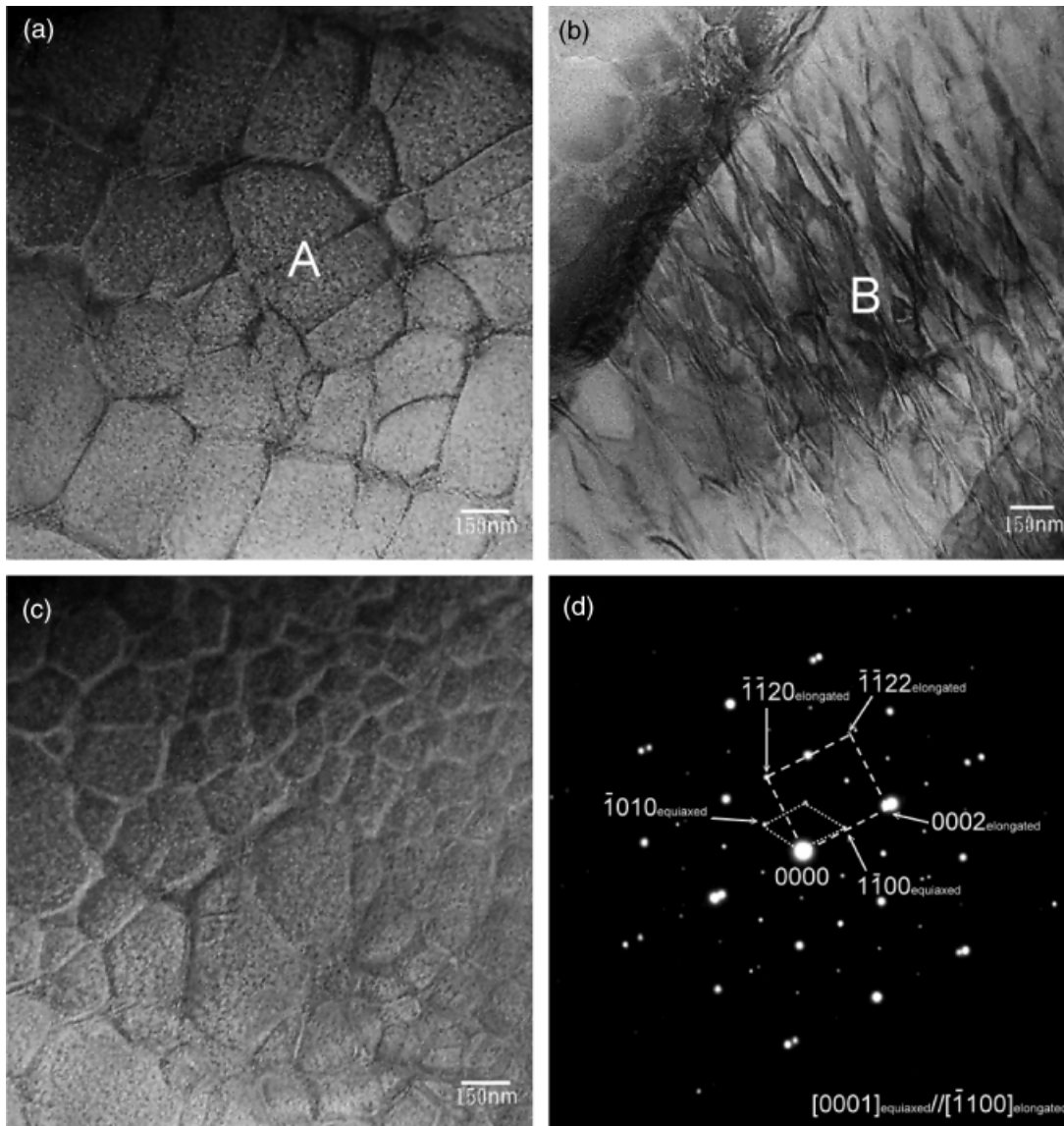


Fig. 3. After annealing at 1300°C for 3 h: (a) bright-field (BF) image of the equiaxed α_2 -Ti₃Al (abutting the τ_1 -Ti₃AlN layer in Fig. 1(a)); (b) BF image of the elongated α_2 -Ti₃Al (abutting the two-phase (α_2 -Ti₃Al+ α -Ti) layer in Fig. 1(a)); (c) variation in the grain size of the equiaxed α_2 -Ti₃Al along the direction from the AlN side (bottom) to the Ti side (top); (d) selected area diffraction pattern of both elongated and equiaxed α_2 -Ti₃Al, showing the orientation relationship of $[0001]_{\text{equiaxed}} // [\bar{1}100]_{\text{elongated}}$ and $(\bar{1}010)_{\text{equiaxed}} // (\bar{1}\bar{1}22)_{\text{elongated}}$.

III. Results and Discussion

The products formed in the AlN/Ti interfacial reaction zone are listed in Table I, after annealing at 1300°–1500°C for various periods. The reaction zone consisted of TiN, τ_2 -Ti₂AlN, τ_1 -Ti₃AlN, α_2 -Ti₃Al, and a two-phase (α_2 -Ti₃Al+ α -Ti) region in sequence after annealing at 1300°C. The γ -TiAl and a lamellar two-phase (γ -TiAl+ α_2 -Ti₃Al) structure were found instead of τ_1 -Ti₃AlN in between τ_2 -Ti₂AlN and α_2 -Ti₃Al after annealing at 1400°C. In comparison with the results after annealing at 1400°C, γ -TiAl was not formed at the interface after annealing at 1500°C. It was noted that there were some exceptions for the initial transition stage. For instance, no τ_2 -Ti₂AlN had been found after annealing at 1350°C for 0.5 h, while γ -TiAl and the lamellar two-phase (γ -TiAl+ α_2 -Ti₃Al) layer did not exist after annealing at 1400°C for 0.5 h, whereas a layer of γ -TiAl was found after annealing at 1500°C for 0.5 h. In contrast to the reaction of AlN and α -Ti thin films annealed at lower temperatures (e.g., 600°–800°C),^{23,24} no TiAl₃ was found in the present study.

(1) SEM/EDS Analyses

Figure 1 shows the secondary electron images of the cross-sectional microstructures of the AlN/Ti diffusion couples after

annealing at various temperatures for 36 h. Figure 1(a) displays that the reaction zone between AlN and Ti consists of TiN, τ_2 -Ti₂AlN, τ_1 -Ti₃AlN, α_2 -Ti₃Al, and a two-phase (α_2 -Ti₃Al+ α -Ti) region in sequence after annealing at 1300°C for 36 h. The microstructure of AlN/Ti after annealing at 1400°C for 36 h is demonstrated in Fig. 1(b), which displays the reaction phase sequence of TiN/ τ_2 -Ti₂AlN/ γ -TiAl/(γ -TiAl+ α_2 -Ti₃Al)/ α_2 -Ti₃Al/(α_2 -Ti₃Al+ α -Ti). The γ -TiAl layer and lamellar structure (γ -TiAl+ α_2 -Ti₃Al), instead of Ti₃AlN, were formed between the Ti₂AlN and Ti₃Al. Figure 1(c) displays the reaction phase sequence of TiN/ τ_2 -Ti₂AlN/(γ -TiAl+ α_2 -Ti₃Al)/ α_2 -Ti₃Al/(α_2 -Ti₃Al+ α -Ti). The TiAl layer was not found at the interface after annealing at 1500°C for 36 h as mentioned above.

El-Sayed *et al.*²⁵ found that the sequence of the reaction layer was AlN/TiN/ τ_1 -Ti₃AlN/ α_2 -Ti₃Al/ α -Ti. However, they did not observe the lamellar two-phase (γ -TiAl+ α_2 -Ti₃Al) and (α_2 -Ti₃Al+ α -Ti) layers. Paransky *et al.*^{26–28} showed that the sequence of TiN, τ_1 -Ti₃AlN, and α_2 -Ti₃Al was formed at the interface of Ti (matrix) and AlN (particle) and that the TiN and τ_1 -Ti₃AlN exhibited a complex interpenetrating morphology. Furthermore, a lamellar two-phase region was also observed between τ_1 -Ti₃AlN and α_2 -Ti₃Al layers after annealing at 1000° and 1100°C. However, in the present study, τ_2 -Ti₂AlN and a

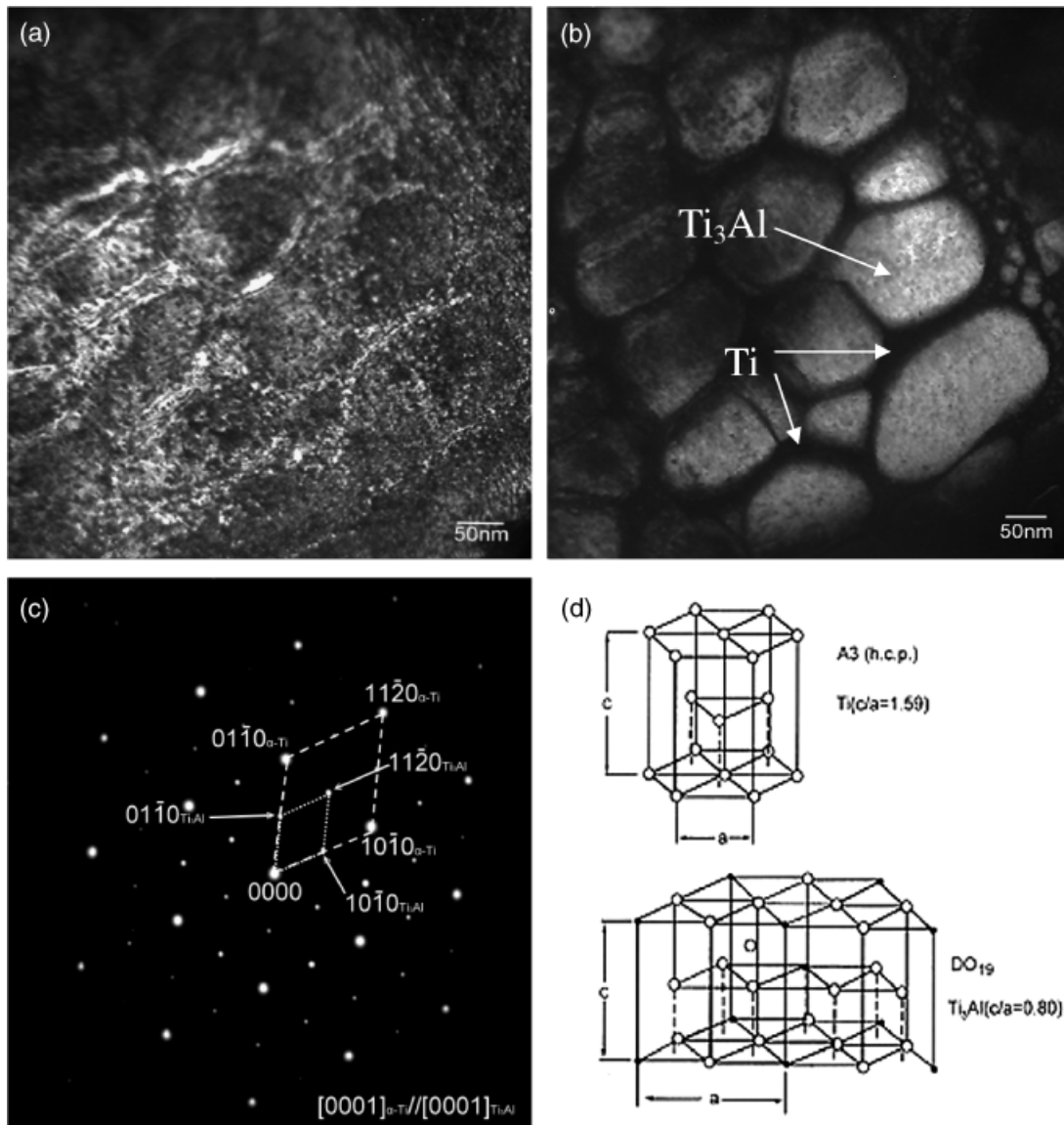


Fig. 4. After annealing at 1300°C for 3 h: (a) bright-field (BF) image of the two-phase (α_2 -Ti₃Al+ α -Ti) region in Fig. 1(a); (b) dark-field (DF) image of α_2 -Ti₃Al formed by the (1120)_{Ti₃Al} diffraction spot; (c) superimposed selected area diffraction patterns obtained from the two-phase (α_2 -Ti₃Al+ α -Ti) region, showing the orientation relationship of [0001] _{α -Ti}//[0001]_{Ti₃Al} and (1100) _{α -Ti}//(1100)_{Ti₃Al}; (d) schematic illustration of α -Ti and α_2 -Ti₃Al crystal structure.

two-phase (α_2 -Ti₃Al+ α -Ti) region existed at the interface after annealing at 1300°C, while γ -TiAl and a lamellar structure (γ -TiAl+ α_2 -Ti₃Al) were found in the interface at 1400°C. In the temperature range used in this study, two lamellar layers were found: one layer (α -Ti+ α_2 -Ti₃Al) was developed because of the precipitation of α_2 -Ti₃Al from α -Ti; the other layer (α_2 -Ti₃Al+ γ -TiAl) was formed because of the eutectoid reaction (α -Ti \rightarrow α_2 -Ti₃Al + γ -TiAl) during cooling.

In Fig. 1, the nitride layers, e.g., TiN, τ_2 -Ti₂AlN, and τ_1 -Ti₃AlN, were so brittle that there were cracks in these layers. The crack formation was attributed to the mismatch of thermal expansion coefficients between aluminum nitride and titanium, resulting in a significant residual thermal stress.

It was also noted that there existed some pores in aluminide layers (i.e., γ -TiAl, α_2 -Ti₃Al, etc.) of the reaction zone. These pores were caused because of the formation of nitrogen bubbles during cooling. A significant amount of nitrogen was dissolved in aluminide layers on heating. However, the solubility of nitrogen in aluminide layers sharply decreased with decreasing temperature, so that nitrogen was supersaturated. The nitrogen bubbles were thus precipitated through a nucleation and growth mechanism like the gas bubble formation commonly encountered in the casting of alloys. It is worth noting that the decrease in the solubility of nitrogen, not the solubility itself, gave rise to

the precipitation of nitrogen bubbles or pores during cooling. This is the reason why nitrogen bubbles primarily existed in α_2 -Ti₃Al, although the solubility of nitrogen in α_2 -Ti₃Al is much larger than that in γ -TiAl. Like the existence of spherical oxygen bubbles in Ti because of the Ti/ZrO₂ interfacial reaction,²⁹ nitrogen bubbles were formed in α -Ti even though the α -Ti is capable of dissolving a large amount of oxygen. On comparing Figs. 1(a)–(c), it was concluded that the amount of bubbles increased with annealing temperature.

(2) TEM/EDS Analyses

Figure 2(a) shows the bright-field (BF) image of the AlN/Ti interface after annealing at 1300°C for 3 h, showing the phases of TiN, τ_2 -Ti₂AlN, τ_1 -Ti₃AlN, and α_2 -Ti₃Al. Note that the two-phase (α_2 -Ti₃Al+ α -Ti) region has not been shown in Fig. 2(a). As shown in Fig. 2(b), the selection area diffraction pattern (SADP) of TiN was indexed as a cubic unit cell with lattice parameters of $a = 0.426$ nm. The TEM/EDS analyses revealed that the layers of τ_2 -Ti₂AlN and τ_1 -Ti₃AlN were ternary compounds with the approximate compositions Ti:Al:N = 2:1:1 and Ti:Al:N = 3:1:1, respectively. The first extensive study of phase equilibria in the Ti–Al–N system was conducted by Schuster and Bauer,³⁰ with two isothermal sections at 1000° and 1300°C being

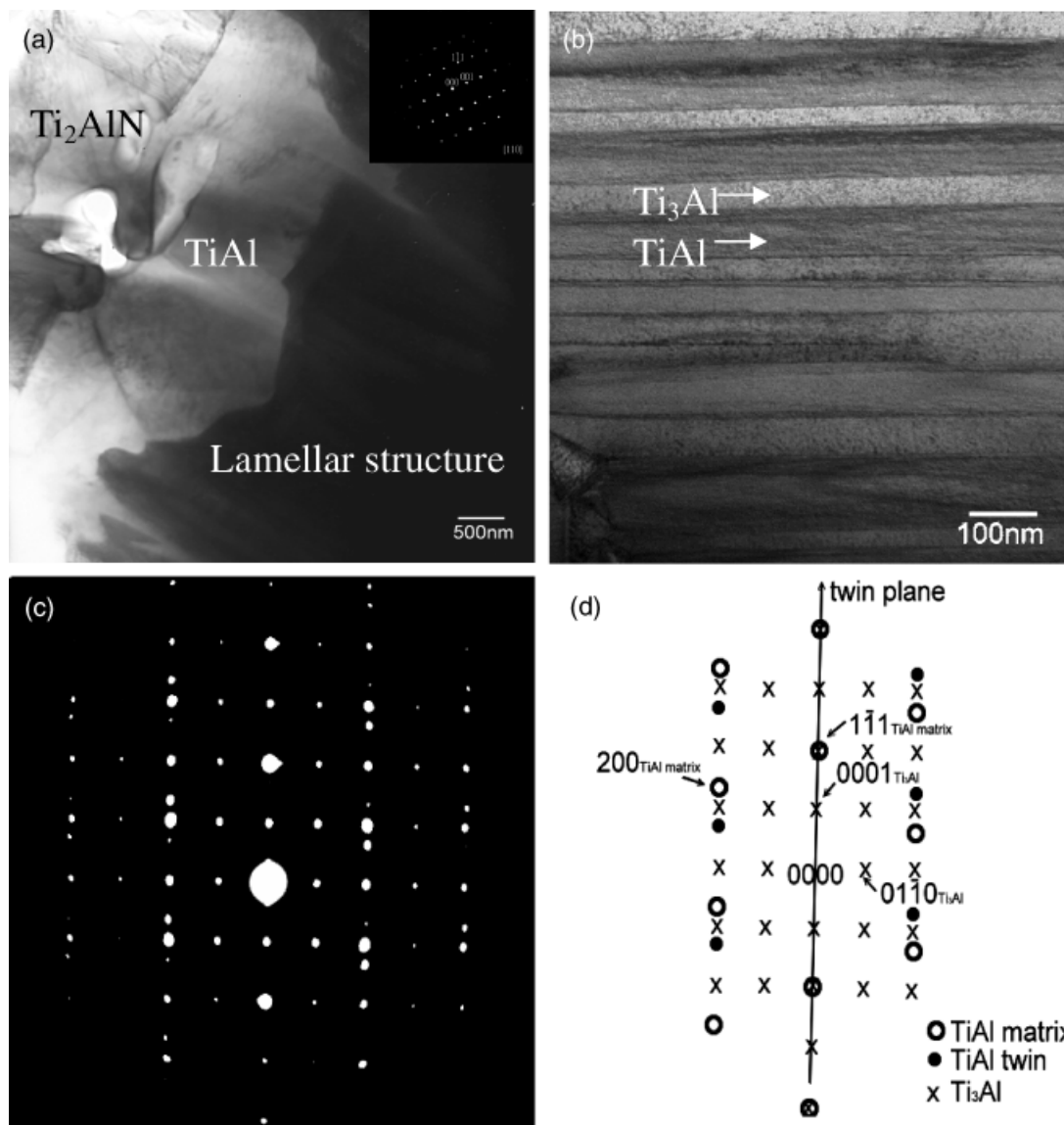


Fig. 5. (a) Bright-field (BF) image of γ -TiAl between the τ_2 -Ti₂AlN and the lamellar structure after annealing at 1500°C/0.5 h; (b) BF image of the lamellar two-phase (γ -TiAl + α_2 -Ti₃Al) structure; (c) superimposed selected area diffraction patterns (SADPs) of γ -TiAl ($Z = [011]$) and ($Z = Z = [2\bar{1}10]$) from the lamellar structure region, showing the orientation relationship of $[011]_{\text{TiAl}} // [2\bar{1}10]_{\text{Ti}_3\text{Al}}$; (d) schematic illustration of the SADPs in (c).

published. Recently, Pietzka and Schuster³¹ showed that three ternary nitride phases Ti₃Al₂N₂, Ti₂AlN_{1-x}, and Ti₃AlN_{1-x} are present in a much more detailed section at 1300°C. The SADPs of τ_2 -Ti₂AlN and τ_1 -Ti₃AlN are shown in Figs. 2(c) and (d), respectively. On indexing these SADPs, it was found that τ_2 -Ti₂AlN had a hexagonal crystal structure with the lattice parameters $a = 0.299$ nm and $c = 1.361$ nm, while the τ_1 -Ti₃AlN was indexed to be a cubic unit cell with the lattice parameter $a = 0.4284$ nm.

The α_2 -Ti₃Al layer, as shown in Figs. 1(a) and 2(a), displayed two distinct features, whose BF images are displayed in Figs. 3(a) and (b), respectively. The α_2 -Ti₃Al layer had two different morphologies, i.e., equiaxed α_2 -Ti₃Al and elongated α_2 -Ti₃Al. Both equiaxed α_2 -Ti₃Al and elongated α_2 -Ti₃Al had the same crystal structure but with different compositions (the Al concentrations ranging from 22 to 39 at. %). The equiaxed structure marked “A” in Fig. 3(a) was corresponding to the regions also marked as “A” in Figs. 1(a) and 2(a), respectively. In the same way, the elongated texture structure marked “B” in Fig. 3(b) was corresponding to the regions both marked as “B” in Figs. 1(a) and 2(a). The EDS quantitative analyses indicated that the equiaxed α_2 -Ti₃Al in Fig. 3(a) and elongated α_2 -Ti₃Al in Fig. 3(b) were 66.90 at. % Ti, 25.07 at. % Al, 8.03 at. % N, and 62.21 at. % Ti, 23.42 at. % Al, and 14.37 at. % N, respectively.

The elongated α_2 -Ti₃Al grains in Fig. 3(b) were well aligned nearly perpendicular to the interface of AlN/Ti. As Al and N diffuse much faster than Ti, the Ti region will be subjected to a state of compression because of the interdiffusion. However, the fact that the equiaxed α_2 -Ti₃Al became elongated along the direction perpendicular to the interface is attributed to the mismatch in the thermal expansion coefficient between AlN and Ti.

Based upon our TEM investigation, the equiaxed α_2 -Ti₃Al was not randomly oriented, because it displayed the same contrast when the specimen was tilted. The equiaxed α_2 -Ti₃Al in Fig. 3(a) was likely to be formed by recrystallization. Previous studies have reported that the α_2 -Ti₃Al alloys could exhibit admirable superplasticity of elongation greater than 1200% at temperatures between 960° and 1000°C and strain rates between 10^{-4} and 10^{-5} s⁻¹.^{32,33} It is believed that the large deformation of textured α_2 -Ti₃Al is likely to trigger the recrystallization. Figure 3(c) displays the variation in the grain sizes of α_2 -Ti₃Al along the direction from the AlN side (bottom) to the Ti side (top). The grain size varies from 150 to 450 nm, implying the different degrees of grain growth after recrystallization. When the α_2 -Ti₃Al, with a deformation texture, was recrystallized, the new equiaxed grains usually had a preferred orientation.³⁴ However, the orientation of the equiaxed α_2 -Ti₃Al was different from that of the textured α_2 -Ti₃Al. The SADP, as shown

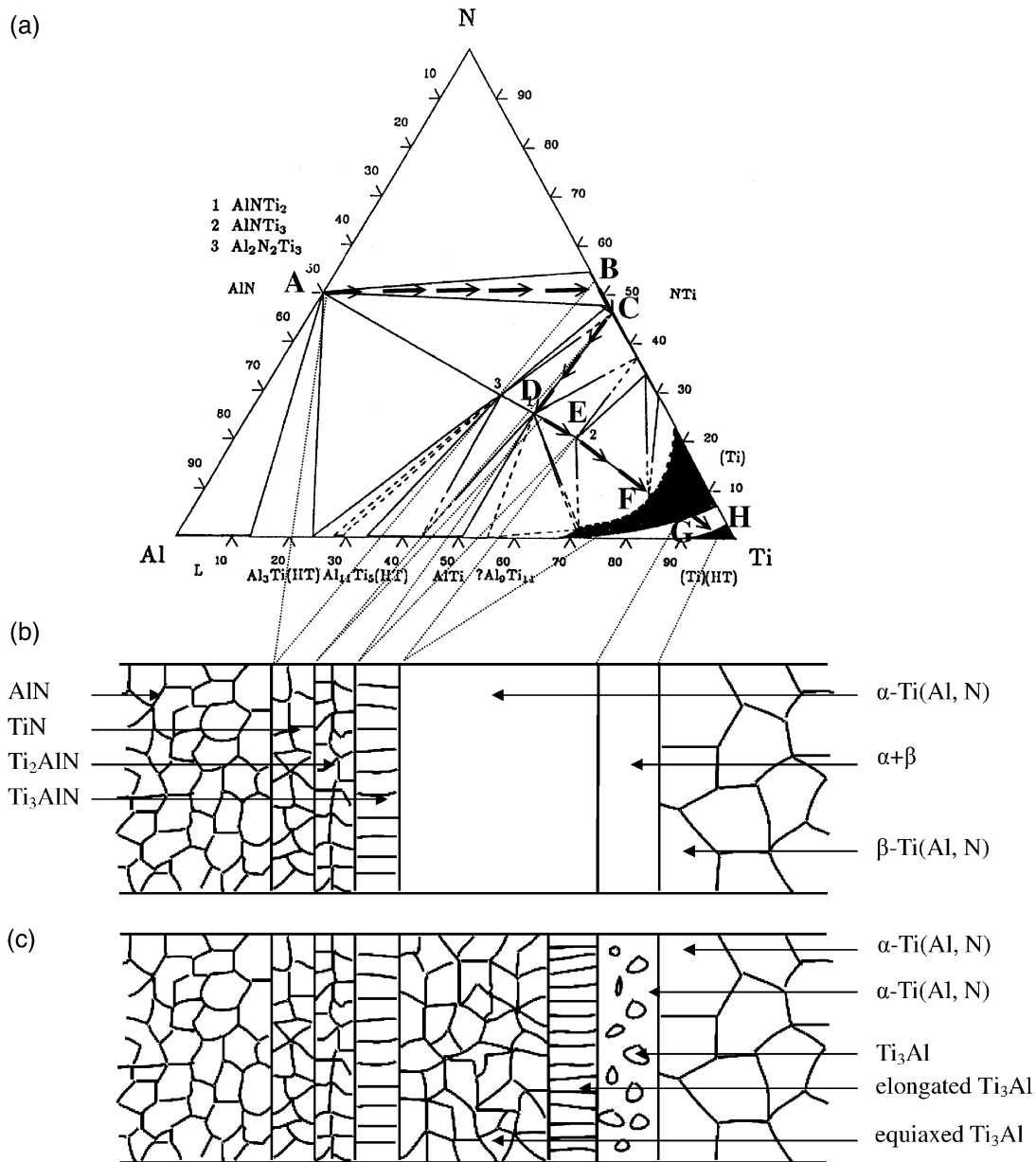


Fig. 6. (a) Isothermal section of the Ti–Al–N phase diagram at 1300°C.³⁰ The diffusion path was drawn as arrows; (b) the microstructure of an AlN/Ti diffusion couple at 1300°C; (c) the microstructure of an AlN/Ti diffusion couple after cooling.

in Fig. 3(d), revealed that the orientation relationship of the equiaxed and the elongated α_2 -Ti₃Al should be as follows: $[0001]_{\text{equiaxed}} // [1100]_{\text{elongated}}$ and $(1010)_{\text{equiaxed}} // (\bar{1}\bar{1}22)_{\text{elongated}}$. The fact that the exquiaxed α_2 -Ti₃Al had a recrystallization texture was because of the influence that the texture of the α_2 -Ti₃Al had on the nucleation and/or growth of the new grains.

Figures 4(a) and (b) show the bright and dark field images of the two-phase (α_2 -Ti₃Al+ α -Ti) layer near the Ti side, respectively. In Fig. 4(b), it can be seen that α -Ti is distributed along the grain boundaries of α_2 -Ti₃Al. The lattice parameters of α -Ti, calculated from the SADPs in Fig. 4(c), were $a = 0.310$ nm and $c = 0.441$ nm, while those of α_2 -Ti₃Al were $a = 0.605$ nm and $c = 0.487$ nm. The a value of α_2 -Ti₃Al was approximately twice that of α -Ti. It was inferred that the α_2 -Ti₃Al was precipitated in the matrix of α -Ti. From the SADPs, where the superlattice diffraction spots of α_2 -Ti₃Al were clearly observed, the α_2 -Ti₃Al precipitates were found to satisfy the following orientation relationship with respect to α -Ti: $[0001]_{\alpha\text{-Ti}} // [0001]_{\text{Ti}_3\text{Al}}$ and $(1\bar{1}00)_{\alpha\text{-Ti}} // (1\bar{1}00)_{\text{Ti}_3\text{Al}}$. The orientation relations are schematically demonstrated in Fig. 4(d).

According to the Ti–Al binary phase diagram,³⁵ α_2 -Ti₃Al was stable up to 1210°C, being a nonstoichiometric compound with a

relatively wide range extending from 23 to 35 at.%. It seemed that α_2 -Ti₃Al could only be formed during isothermal annealing below 1210°C. However, the α_2 -Ti₃Al phase was formed after isothermal annealing at temperatures higher than 1300°C, as mentioned previously. This implied that the α_2 -Ti₃Al precipitated from α -Ti during cooling. The existence of (α -Ti+ α_2 -Ti₃Al), α_2 -Ti₃Al, or (α_2 -Ti₃Al+ γ -TiAl) various aluminide layers in the reaction zone of the AlN–Ti diffusion couple, which was isothermally annealed above 1300°C, can be explained by a modified Ti–Al binary phase diagram, and will be described afterwards.

Figure 5(a) shows the BF image of the AlN/Ti interfacial reaction zone after annealing at 1500°C for 0.5 h, showing τ_2 -Ti₂AlN, γ -TiAl, and the two-phase (γ -TiAl+ α_2 -Ti₃Al) layer. The inset on the upper right corner shows the SADP of γ -TiAl with the zone axis of [110]. The (γ -TiAl+ α_2 -Ti₃Al) lamellar structure is displayed at a higher magnification in Fig. 5(b). The two-phase (γ -TiAl+ α_2 -Ti₃Al) region usually forms a lamellar morphology consisting of colonies of thin parallel α_2 -Ti₃Al and γ -TiAl platelets. Based upon the Ti–Al phase diagram, the lamellar structure resulted from the eutectoid reaction of $\alpha \rightarrow \alpha_2 + \gamma$. From the SADPs of the lamellar structure (Fig. 5(c)) and its corresponding schematic diagram (Fig. 5(d)), the

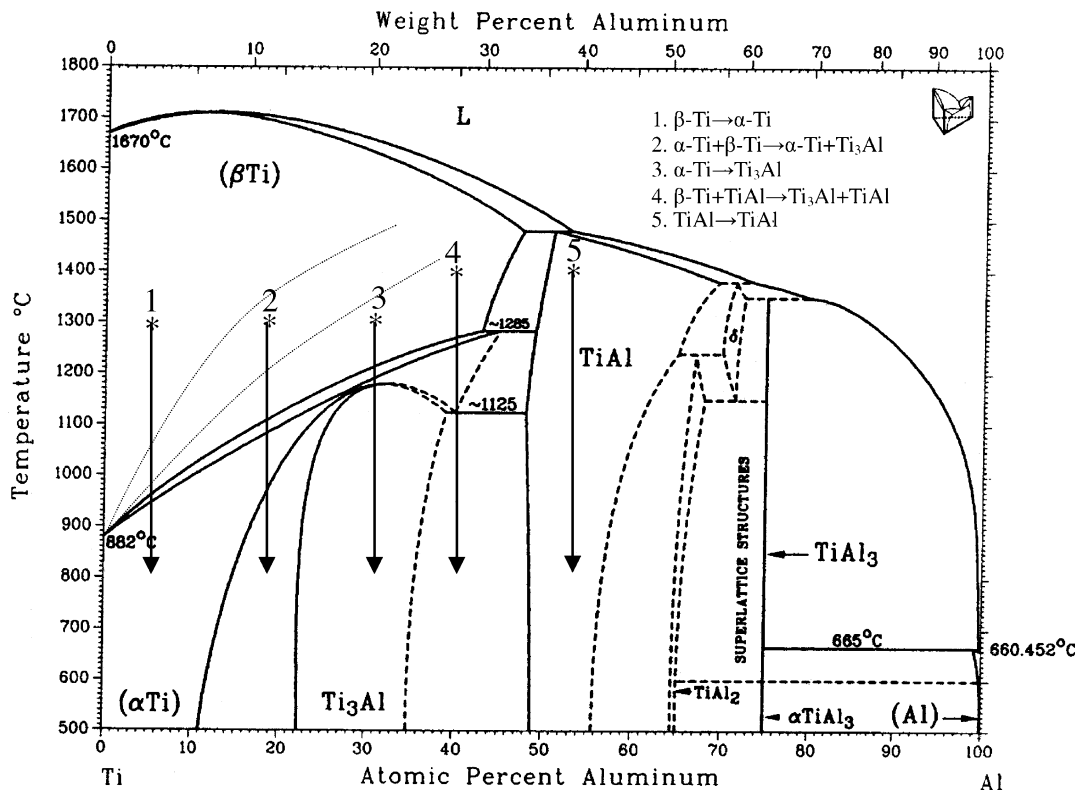


Fig. 7. A modified Ti-Al phase diagram because of the stabilization of α -Ti by dissolving N (see the dashed line),³⁵ showing the cooling processes of the various aluminides after annealing at 1300°C (lines 1-3) and at 1400°C (lines 4 and 5). The increase in the $\alpha \rightarrow \beta$ transformation temperature has been exaggerated for clarification.

orientation relationship of γ -TiAl and α_2 -Ti₃Al was identified: $[011]_{\text{TiAl}} // [2\bar{1}10]_{\text{Ti}_3\text{Al}}$ and $(111)_{\text{TiAl}} // (01\bar{1}0)_{\text{Ti}_3\text{Al}}$. In addition, the schematic SADP patterns in Fig. 5(d) show some extra spots caused by the structure of twinning in tetragonal crystals of γ -TiAl. The matrix of γ -TiAl was oriented with its $[011]$ zone axis parallel to the electron beam, while the twinning plane $(1\bar{1}1)$, was in the edge-on direction along the electron beam. The diffraction patterns of the matrix and the twin were related by a mirror reflection across the $(1\bar{1}1)$ twinning plane or by a rotation of 180° around the normal to the twinning plane.

(3) Microstructural Development and Diffusion Path at 1300°C

When Ti comes into contact with AlN, the system becomes unstable. It is generally acknowledged that the interfacial reactions between Ti and AlN include the following steps. AlN is reduced under the effect of Ti at the annealing temperature. The decomposed Al and N atoms then diffuse into the Ti, and they react with each other to produce binary or ternary nitrides and aluminides. While the nitrides are stable during the subsequent cooling, the aluminides will be subjected to phase transformation based on the Ti-Al binary phase diagram.

Figure 6 illustrates the relationship between the Ti-Al-N phase diagram³⁰ and the microstructure developed in the Ti/AlN diffusion couple, which was isothermally annealed at 1300°C. Figure 6(a) illustrates the isothermal section of the Ti-Al-N ternary phase diagram at 1300°C. Based on the experimental results, it is proposed that the diffusion path, indicative of the compositions along the longitudinal direction perpendicular to the interface, was A-B-C-D-E-F-G-H when the diffusion couple was annealed at 1300°C.

It is worth noting that the diffusion path is deviated from the ideal direct path between the compositions of the end points, i.e., Ti and AlN, as the diffusion velocities of the Ti, Al, and N atoms are significantly different in the Ti-AlN diffusion couple. The radii of N, Ti, and Al atoms are 0.07, 0.1448, and 0.1431

nm, respectively, so that N atoms, diffusing interstitially in the Ti, should have a higher diffusion velocity than that of Al atoms, which diffuse mainly by substitution. In the literature, the diffusion coefficients of Al and N atoms in Ti are reported to be 7.4×10^{-7} cm²/s at 600–850°C and 1.2×10^{-2} cm²/s at 900–1570°C, respectively.^{36,37} Thus the TiN layer will firstly be formed at the interface, leading to the deviation of the diffusion path toward the TiN end (edge BC in Fig. 6(a)). As TiN has a wide range of nitrogen solubility and hardly dissolves Al atoms, much more Al atoms than N atoms will diffuse into the titanium side beyond the TiN layer, resulting in the formation of τ_2 -Ti₂AlN, τ_1 -Ti₃AlN, and various aluminide layers.

The diffusion path crosses the fields of AlN+TiN, TiN, TiN+ τ_2 -Ti₂AlN, τ_2 -Ti₂AlN+ τ_1 -Ti₃AlN, τ_1 -Ti₃AlN+ α -Ti, α -Ti, α -Ti+ β -Ti, and β -Ti. The tie lines of the ternary phase diagram correspond to the interface of two reaction layers in the diffusion couple, similar to the case for the interface between carbon and titanium aluminides presented by Viala *et al.*³⁸ As shown in Fig. 6(b), the layers of TiN, τ_2 -Ti₂AlN, τ_1 -Ti₃AlN, α -Ti(Al,N), α -Ti(Al,N)+ β -Ti(Al,N), and β -Ti(Al,N) will be formed in sequence from AlN to Ti at the annealing temperature (1300°C).

Figure 6(c) shows the microstructure formed during the cooling stage. It is believed that the nitride layers, including TiN, τ_2 -Ti₂AlN, and τ_1 -Ti₃AlN, remained during cooling. However, the aluminide layers (i.e., α -Ti(Al,N), α -Ti(Al,N)+ β -Ti(Al,N), and β -Ti(Al,N)) were subjected to phase transformation during the subsequent cooling, causing the formation of the α_2 -Ti₃Al layer and the lamellar two-phase (α_2 -Ti₃Al+ α -Ti) layer.

The phase transformation of aluminides, mentioned above, can be shown schematically in the Ti-Al binary phase diagram as shown in Fig. 7. Because nitrogen is an α -Ti stabilizers, the β / $(\alpha+\beta)$ and $(\alpha+\beta)$ / α boundaries of the Ti-Al binary phase diagram are shifted upward by dissolving N atoms. The β -Ti layer abutting the reaction-unaffected Ti, with a small amount of Al and N in solid solution, was transformed into α -Ti on cooling, as indicated by line 1 in Fig. 7. The α -Ti+ β -Ti layer at 1300°C was transformed into the α -Ti+ α_2 -Ti₃Al layer after cooling (line

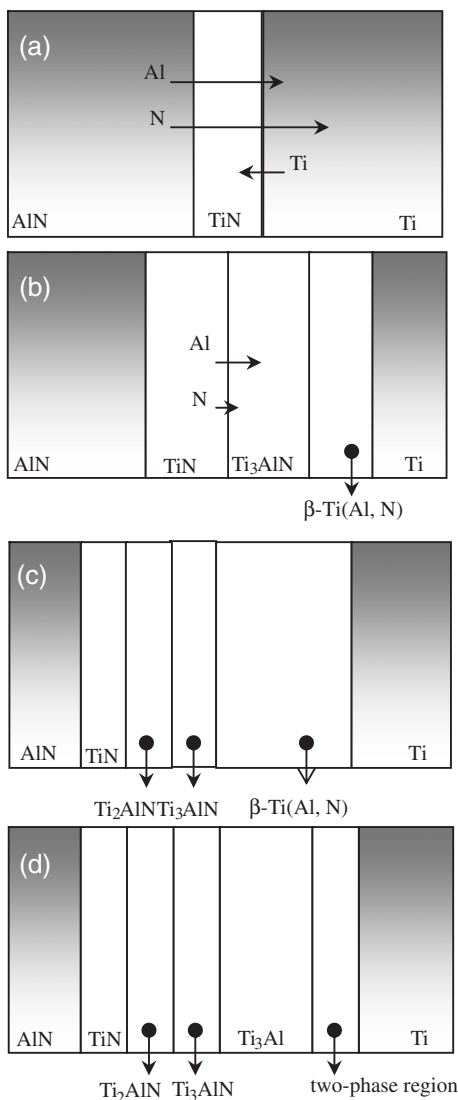


Fig. 8. Proposed reaction mechanisms of the AlN and Ti diffusion couple annealed at 1300°C: (a) first stage: formation of TiN; (b) second stage: formation of τ_1 -Ti₃AlN, α -Ti(Al,N)+ β -Ti(Al,N), and α -Ti(Al,N); (c) third stage: formation of τ_2 -Ti₂AlN; (d) fourth stage: formation of α_2 -Ti₃Al and/or the two-phase layer (α_2 -Ti₃Al+ α -Ti) during cooling. (τ_1 :Ti₃AlN; τ_2 :Ti₂AlN; α_2 :Ti₃Al; α :hexagonal Ti(Al,N); β : cubic Ti(Al,N).

2 in Fig. 7), while the α -Ti layer was transformed into α_2 -Ti₃Al (line 3 in Fig. 7).

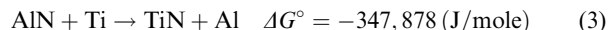
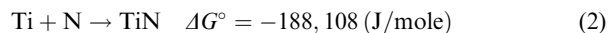
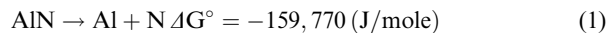
For comparison, a α -Ti layer and/or a γ -TiAl layer with a higher Al content were likely formed when the diffusion couple was isothermally annealed at temperatures higher than 1300°C. Thus, more aluminate layers, including the two-phase (γ -TiAl+ α_2 -Ti₃Al) layer and/or γ -TiAl layer, could exist in the Ti/AlN diffusion couple because of the more extensive Al diffusion after annealing at 1400° or 1500°C. After isothermal annealing at 1400°C, the α -Ti layer with a high Al content underwent the following reaction: α -Ti \rightarrow γ -TiAl+ α_2 -Ti₃Al as indicated by line 4 in Fig. 7, while the γ -TiAl layer still remained as it was on cooling (line 5 in Fig. 7). It is worth noting that no γ -TiAl existed in the diffusion couple after annealing at 1500°C. After TiN_{1-x} was saturated in N at such a high temperature, the excess nitrogen would diffuse from the TiN_{1-x} layer, resulting in the nitridization of γ -TiAl, that is τ_2 -Ti₂AlN.

(4) Reaction Zone Growth Mechanisms at 1300°C

Based upon the results and the discussion mentioned above, an attempt was made to propose an interfacial reaction model between AlN and Ti. The formation mechanisms for several dif-

ferent stages at 1300°C, as an example, are schematically shown in Fig. 8.

(A) *First Stage: Formation of TiN:* In the first stage, AlN decomposes at the original AlN/Ti interface into Al and N under the effect of Ti. As Ti has a strong affinity with N, the fast diffusion species N atoms will go into Ti, leading to the formation of TiN with Al in solid solution. The formation of TiN in the initial stage can be expressed by the following reactions, as shown in Fig. 8(a).³⁹



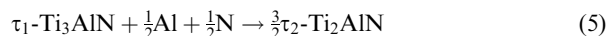
The diffusion of N atoms and Al atoms in TiN is much faster than that of Ti atoms in AlN (diffusivities of N and Al in TiN are $5.4 \times 10^{-3} \text{ cm}^2/\text{s}$ at 1000°–1500°C and $3 \times 10^{-14} \text{ cm}^2/\text{s}$ at 300°–550°C; the diffusivity of Ti in AlN is 4×10^{-17} at 1280°–1400°C).⁴⁰ Thus, Al and N continuously diffuse through the TiN layer and reaction (2) takes place at the interface of TiN and Ti. The highly negative Gibbs free energy change of the reaction (3) indicates that the reaction between aluminum nitride and titanium is thermodynamically favorable.

(B) *Second Stage: Formation of Ti₃AlN and Various Titanium Aluminides:* When the concentrations of Al and N increase to a certain amount, τ_1 -Ti₃AlN is formed, as shown in Fig. 8(b), at the interface of TiN/Ti according to the following reaction:

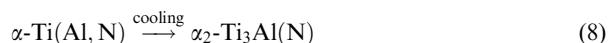
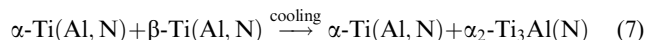
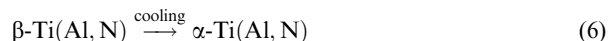


The formation of τ_1 -Ti₃AlN instead of τ_2 -Ti₂AlN at this stage is consistent with the fact that τ_1 -Ti₃AlN was found after annealing at 1300°C/0.5 h, which was at a relatively early stage. Meanwhile, excess Al and N atoms further go into Ti as a solid solution, leading to the formation of various titanium aluminonitrides, for example, α -Ti(Al,N) and the α -Ti(Al,N)+ β -Ti(Al,N) two-phase region.

(C) *Third Stage: Formation of Ti₂AlN:* As shown in Fig. 8(c), τ_2 -Ti₂AlN is formed at this stage. The growth of the τ_2 -Ti₂AlN was controlled by the diffusion of Al and N through TiN, accumulating at the TiN/ τ_1 -Ti₃AlN interface, leading to the disappearance of τ_1 -Ti₃AlN based upon the following reaction:



(D) *Fourth Stage: Formation of α_2 -Ti₃Al and/or the Two-Phase Layer (α_2 -Ti₃Al+ α -Ti) During Cooling:* Figure 8(d) shows that the α -Ti(Al,N)+ β -Ti(Al,N) two-phase region was transformed into the (α_2 -Ti₃Al+ α -Ti) two-phase layer, while the α -Ti(Al,N) layer was transformed into the α_2 -Ti₃Al layer during cooling, depending upon the local composition. Not shown in Fig. 8(d) is that the β -Ti(Al,N) was transformed into the α -Ti(Al,N). The phase transformations mentioned above can be expressed by the following reactions,



IV. Conclusions

1. An interfacial reaction zone, consisting of TiN, τ_2 -Ti₂AlN, τ_1 -Ti₃AlN, α_2 -Ti₃Al, and a two-phase (α_2 -Ti₃Al+ α -Ti) region in sequence, was observed in between AlN and Ti after annealing at 1300°C.

2. After annealing at 1300°C, a textured structure existed in the α_2 -Ti₃Al layer probably because of the internal stresses resulting from the mismatch in the thermal expansion coefficient between AlN and Ti. The fine equiaxed α_2 -Ti₃Al grains implied the occurrence of recrystallization. The orientation relationship between the equiaxed and elongated α_2 -Ti₃Al was as follows: $[0001]_{\text{equiaxed}} // [\bar{1}100]_{\text{elongated}}$ and $(\bar{1}010)_{\text{equiaxed}} // (\bar{1}\bar{1}22)_{\text{elongated}}$.

3. In the two-phase (τ_1 -Ti₃AlN+ α -Ti) region after annealing at 1300°C, α_2 -Ti₃Al and α -Ti were found to satisfy the following orientation relationship: $[0001]_{\alpha\text{-Ti}} // [0001]_{\text{Ti}_3\text{Al}}$ and $(\bar{1}\bar{1}00)_{\alpha\text{-Ti}} // (\bar{1}\bar{1}00)_{\text{Ti}_3\text{Al}}$. The a value of α_2 -Ti₃Al was approximately twice that of α -Ti.

4. The γ -TiAl and a lamellar two-phase (γ -TiAl+ α_2 -Ti₃Al) structure were found in between τ_2 -Ti₂AlN and α_2 -Ti₃Al after annealing at 1400°C. The orientation relationship of γ -TiAl and α_2 -Ti₃Al in the lamellar structure was identified to be as follows: $[2\bar{4}2\bar{3}]_{\text{Ti}_3\text{Al}} // [012]_{\text{TiAl}}$ and $(10\bar{1}0)_{\text{Ti}_3\text{Al}} // (100)_{\text{TiAl}}$. Compared with the results after the reaction at 1400°C, γ -TiAl was not formed at the interface after the reaction at 1500°C.

5. The diffusion path, connecting the phases formed by the reaction between AlN and Ti, was drawn on the Ti–Zr–O ternary phase diagram. Furthermore, the relationships among the Ti–Al–N ternary phase diagram, a modified binary phase diagram, and the microstructural development between AlN and Ti at 1300°C and subsequent cooling have been proposed.

References

- ¹C. A. Slack, "Nonmetallic Crystals with High Thermal Conductivity," *J. Phys. Chem. Solids*, **34**, 321–35 (1973).
- ²N. Iwase, K. Anzai, and K. Shinozaki, "Aluminum Nitride Substrates Having High Thermal Conductivity," *Toshiba Rev.*, **153**, 49–53 (1985).
- ³P. Martineau, R. Pailler, M. Lahaye, and R. Naslain, "SiC Filament/Titanium Matrix Composites Regarded as Model Composites. II—Fiber/Matrix Chemical Interactions at High Temperatures," *J. Mater. Sci.*, **19**, 2749–70 (1984).
- ⁴J. C. Feng, M. Naka, and J. C. Schuster, "Reaction Mechanism Between SiC Ceramic and Titanium Foil in Solid State Bonding," *J. Jpn. Inst. Metals*, **59**, 978–83 (1995).
- ⁵W. J. Whatley and F. E. Wawner, "Kinetics of the Reaction Between SiC (SCS-6) Filaments and Titanium (6Al–4V) Matrix," *J. Mater. Sci. Lett.*, **4** [2] 173–5 (1985).
- ⁶D. Travessa and M. Ferrante, "The Al₂O₃–Titanium Adhesion in the View of the Diffusion Bonding Process," *J. Mater. Sci.*, **37**, 4385–90 (2002).
- ⁷R. Yue, Y. Wang, C. Chen, and C. Xu, "Interface Reaction of Ti and Mullite Ceramic Substrate," *Appl. Surf. Sci.*, **126**, 255–64 (1998).
- ⁸E. Faran, I. Gotman, and E. Y. Gutmanas, "Experimental Study of the Reaction Zone at Boron Nitride Ceramic–Ti Metal Interface," *Mater. Sci. Eng.*, **A288**, 66–74 (2000).
- ⁹K. L. Lin and C. C. Lin, "Ti₂ZrO Phases Formed in the Titanium and Zirconia Interface after Reaction at 1550°C," *J. Am. Ceram. Soc.*, **88** [5] 1268–72 (2005).
- ¹⁰P. A. Janeway, "Making the Grade in Demanding Electronic Application," *Ceram. Ind.*, **137**, 28–32 (1991).
- ¹¹J. A. Chediak, "Ceramic Engineers in the 21st Century," *Am. Ceram. Soc. Bull.*, **75** [1] 52–5 (1996).

- ¹²T. B. Jackson, A. V. Virkar, K. L. More, R. B. Dinwiddie, and R. A. Cutler, "High-Thermal-Conductivity Aluminum Nitride Ceramics: The Effect of Thermodynamic, Kinetic and Microstructural Factors," *J. Am. Ceram. Soc.*, **80** [6] 1421–35 (1997).
- ¹³S. Nakahata, K. Sogabe, T. Matsuura, and A. Yamakawa, "One Role of Titanium Compound Particles in Aluminum Nitride Sintered Body," *J. Mater. Sci.*, **32**, 1873–6 (1997).
- ¹⁴H. D. Lee, "Phase Chemistry, Thermodynamic and Kinetic Characterization of Interfacial Reaction Between Aluminum Nitride and Titanium"; Ph.D. Dissertation, Arizona State University, Tempe, AZ, 1993.
- ¹⁵A. D. Westwood and M. R. Notis, "Analytical Electron Microscopy Study of AlN Substrates and Metallization Interfaces," *Adv. Ceram.*, **26**, 171–87 (1989).
- ¹⁶A. D. Westwood and M. R. Notis, "An Issue in Thermal Management: Metallizing High Thermal Conductivity Ceramic Substrates in Microelectronics," *J. Miner. Met. Mater. Soc.*, **43** [6] 10–5 (1991).
- ¹⁷X. He, K. Tao, and Y. Fan, "Solid-State Reaction of Ti and Ni Thin with Aluminum Nitride," *J. Vac. Sci. Technol.*, **14** [4] 2564–9 (1996).
- ¹⁸T. Yasumoto, K. Amakawa, N. Iwase, and N. Shinsawa, "Reaction Between AlN and Metal Thin Films During High Temperature Annealing," *J. Ceram. Soc. Jpn.*, **101** [9] 969–73 (1993).
- ¹⁹Y. Imanaka and M. R. Notis, "Interfacial Reaction Between Titanium Thin Films and Aluminum Nitride Substrates," *J. Am. Ceram. Soc.*, **82** [6] 1547–52 (1999).
- ²⁰A. H. Carim and R. E. Loehman, "Microstructure at the Interface Between AlN and a Ag–Cu–Ti Braze Alloy," *J. Mater. Res.*, **5** [7] 1520–9 (1990).
- ²¹R. E. Loehman, "Interfacial Reactions in Ceramic–Metal Systems," *Ceram. Bull.*, **68** [4] 891–6 (1989).
- ²²R. E. Loehman and A. P. Tomsia, "Reactions of Ti and Zr with AlN and Al₂O₃," *Acta Metall. Mater.*, **40** (Suppl.) S75–83 (1992).
- ²³X. He, S. Z. Yang, K. Tao, and Y. Fan, "Investigation of the Interface Reactions of Ti Thin Films with AlN Substrate," *J. Mater. Res.*, **12** [3] 846–51 (1997).
- ²⁴M. Pinkas, N. Frage, N. Froumin, J. Pelleg, and M. P. Dariel, "Early Stages of Interface Reactions Between AlN and Ti Thin Films," *J. Vac. Sci. Technol.*, **20** [3] 887–96 (2002).
- ²⁵M. H. El-Sayed, M. Naka, and J. C. Schuster, "Interfacial Structure and Reaction Mechanism of AlN/Ti Joints," *J. Mater. Sci.*, **32**, 2715–21 (1997).
- ²⁶Y. Paransky, A. Berner, and I. Gotman, "Microstructure of Reaction Zone at the Ti–AlN Interface," *Mater. Lett.*, **40**, 180–6 (1990).
- ²⁷Y. Paransky, I. Gotman, and E. Y. Gutmanas, "Reactive Phase Formation at AlN–Ti and AlN–TiAl Interfaces," *Mater. Sci. Eng.*, **A277**, 83–94 (2000).
- ²⁸Y. M. Paransky, A. I. Berner, I. Y. Gotman, and E. Y. Gutmanas, "Phase Recognition in AlN–Ti System by Energy Dispersive Spectroscopy and Electron Backscatter Diffraction," *Mikrochim. Acta*, **134**, 171–7 (2000).
- ²⁹K. L. Lin and C. C. Lin, "Zirconia-Related Phases in the Zirconia/Titanium Diffusion Couple after Annealing at 1000°C–1550°C," *J. Am. Ceram. Soc.*, **88** [10] 2928–34 (2005).
- ³⁰J. C. Schuster and J. Bauer, "The Ternary System Titanium–Aluminum–Nitrogen," *J. Solid State Chem.*, **53** [2] 260–5 (1984).
- ³¹M. A. Pietzka and J. C. Schuster, "Phase Equilibria in the Quaternary System Ti–Al–C–N," *J. Am. Ceram. Soc.*, **79** [9] 2321–30 (1996).
- ³²A. Dutta and D. Banerjee, "Superplastic Behaviour in a Ti₃Al–Nb Alloy," *Scripta Metall. Mater.*, **24** [7] 1319–22 (1990).
- ³³J. M. Kim, C. G. Park, T. K. Ha, and Y. W. Chang, "Microscopic Observation of Superplastic Deformation in a 2-Phase Ti₃Al–Nb Alloy," *Mater. Sci. Eng.*, **A269**, 197–204 (1999).
- ³⁴B. D. Cullity, *Elements of X-Ray Diffraction*. Addison-Wesley Publishing Company Inc., California, USA, 1978.
- ³⁵J. L. Murray, *Phase Diagrams of Binary Titanium Alloys*. ASM International, Metals Part, Ohio, USA, 1987.
- ³⁶J. Raisanen, A. Anttila, and J. Keinonen, "Diffusion of Aluminum in Ion-Implanted α -Ti," *J. Appl. Phys.*, **57** [2] 613–4 (1985).
- ³⁷A. Anttila, J. Raisanen, and J. Keinonen, "Diffusion of Nitrogen in α -Ti," *Appl. Phys. Lett.*, **42** [6] 498–500 (1983).
- ³⁸J. C. Viala, N. Peillon, L. Clochefefer, and J. Bouix, "Diffusion Paths and Reaction Mechanisms in the High-Temperature Chemical Interaction Between Carbon and Titanium Aluminides," *Mater. Sci. Eng.*, **A203**, 222–37 (1995).
- ³⁹I. Barin, *Thermochemical Data of Pure Substances*. VCH, Weinheim, Germany, 1993.
- ⁴⁰L. Hultman, "Thermal Stability of Nitride Thin Films," *Vacuum*, **57**, 1–30 (2000). □